Adsorption in Noninterconnected Pores Open at One or at Both Ends: A Reconsideration of the Origin of the Hysteresis Phenomenon

B. Coasne, A. Grosman, C. Ortega, and M. Simon

Groupe de Physique des Solides, Universités Paris 6 et 7, UMR-CNRS 75-88, 2 place Jussieu, 75251 Paris Cedex 05, France

(Received 28 July 2001; published 6 June 2002)

We report on an experimental study of adsorption isotherm of nitrogen onto porous silicon with noninterconnected pores open at one or at both ends in order to check for the first time the old (1938) but always current idea based on Cohan's description which suggests that the adsorption of gas should occur reversibly in the first case and irreversibly in the second one. Hysteresis loops, the shape of which is usually associated with interconnections in porous media, are observed whether the pores are open at one or at both ends, in contradiction with Cohan's model.

DOI: 10.1103/PhysRevLett.88.256102 PACS numbers: 68.43.–h, 05.70.Np, 61.43.Gt, 64.70.Fx

Adsorption isotherms in mesoporous materials exhibit two main typical features: (i) a sharp increase in the amount of gas adsorbed at a pressure below the saturated vapor pressure of the bulk gas which is attributed to capillary condensation in pores of confining sizes; (ii) the desorption process fails to retrace the path of the adsorption one, so that a hysteresis loop appears revealing the irreversibility of the phenomenon.

Zsigmondy [1] proposed the first explanation of the capillary condensation based on the macroscopic Kelvin equation. In order to explain the hysteresis phenomenon, Cohan [2] went further and proposed different scenarios for filling and emptying of a pore which he also described with the macroscopic concept of meniscus. In a cylindrical pore open at both ends, the shape of gas/adsorbate interface is different during the adsorption and desorption processes leading to hysteresis. On the contrary, in a cylindrical pore closed at one end, the adsorption is reversible since the same meniscus is present during the filling and the emptying of the pore.

The irreversibility of the adsorption process in a cylindrical pore open at both ends, expected by Cohan on the basis of thermodynamic considerations, has been predicted by new numerical approaches. Grand canonical Monte Carlo (GCMC) simulations [3] and analytical approaches [4], together with density functional theory (DFT) [5], have also allowed proposing that the hysteresis phenomenon is an intrinsic property of the phase transition in a single idealized pore and arises from the existence of metastable gaslike and/or liquidlike states. No calculations have yet been performed for cylindrical pores closed at one end.

Macroscopic descriptions based on Cohan's model are currently used to describe the adsorption in noninterconnected mesoporous media and in particular to determine the pore size distribution (PSD) via the Barrett-Joyner-Halenda (BJH) method [6].

However, the experimental validation of Cohan's model has never been checked since the synthesis of ordered mesoporous media with noninterconnected pores open at one or at both ends was unsuccessful for a long time. We report in this paper, for the first time, on an experimental investigation of Cohan's predictions, using mesoporous silicon which exhibits two essential properties: (i) the tubular pores are noninterconnected and do not exhibit narrow sections and (ii) it exists under two forms with pores closed at one end when the porous layer is supported by the substrate or open at both ends when the layer is removed from the substrate.

Porous silicon is prepared by electrochemical etching of a Si single crystal in a HF solution. Its morphology depends on the type and concentration of the dopant atoms [7]. The adsorption studies presented here have been performed with porous layers prepared from a highly boron doped [100] Si substrate. The porosity is controlled by the current density and HF concentration, and the thickness by the duration of the anodic dissolution. The pore volume is determined with high precision by weighing the sample before and after the electrochemical dissolution. To calibrate the porosity and thickness of the layer we need a third weighing after the dissolution of the porous part in a NaOH solution. Note that the porous layers are perfectly reproduced. The porous layers under study have a porosity of 51% and the length of the pores is 21 μm.

The morphology of these layers [see Figs. 1(a) and 1(b)] can be described as a honeycomblike structure with pores perpendicular to the Si substrate separated from each other by Si single crystal walls [inset of Fig. 1(b)] of constant thickness ($\sim$5 nm).

The polygonal-shaped pores are of the same length and closed at one end by the Si substrate. At the end of the porous layer formation which takes about 20 min, an increase in the current density leads to the electropolishing regime during which the Si walls at the bottom of the pores are dissolved so that the porous layer comes off the Si substrate. Such a process takes only a few seconds so that the PSD of the porous layer is not changed. Playing with this possibility, a porous Si layer or a porous Si membrane can be obtained with pores open at one or at both ends, respectively.

We have shown that there is no lateral interconnection between the pores in these layers. The method involves deposition by evaporation at ambient temperature, of an

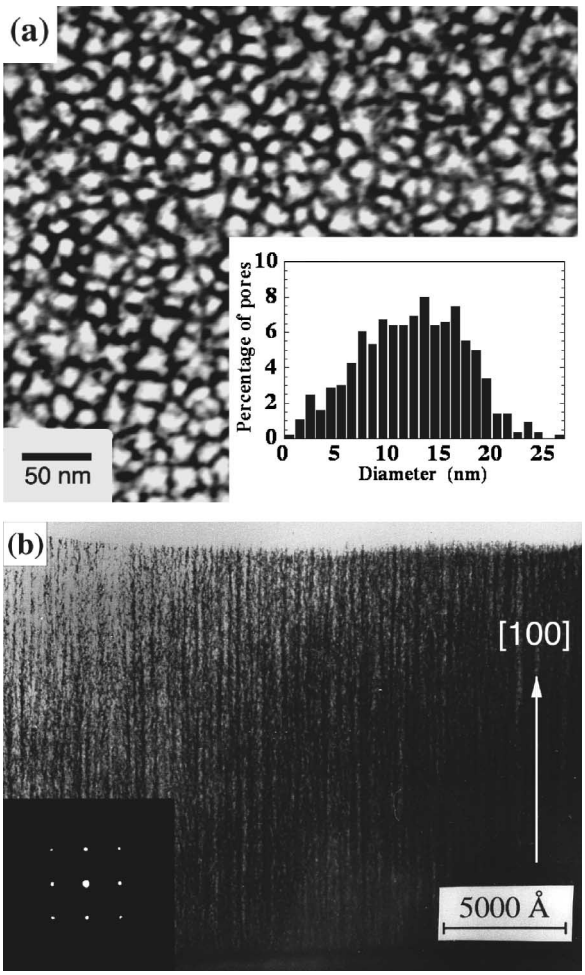

FIG. 1. Bright field TEM images in a plane view (a) and cross section (b) of a porous Si layer with 51% porosity prepared from p^+ type ($\sim 3.10^{-3}\ \Omega \cdot$ cm) [100] Si substrate. Observation axis [100]. Pores (white) are separated by Si walls (black). The pore density is 3.2×10^{11} cm^{-2}. Inset of (a): PSD. Inset of (b): transmission electronic diffraction pattern.

aluminum layer, 500 nm thick, on a part (A_c and B_c) of the top of two porous samples A and B, followed by a thermal annealing under neutral atmosphere of argon at 450 °C for one-half hour to improve the contact between the Al deposit and the silicon. We have shown by Rutherford backscattering analysis with 2 MeV α particles that the Al deposited on the samples is well localized on the top of the pores and constitutes a cap. One of the two samples (A) was thermally oxidized in O_2 enriched in ^{18}O (99%), at 300 °C, 12 mbar, for one hour. This leads to the formation of a thin silicon oxide ($\sim$1 nm) on the silicon walls. The ^{18}O contents in the porous layers under the Al cap (A_c and B_c) and beside it (A_o) were determined by the nuclear reaction $^{18}\mathrm{O}(p,\alpha)^{15}\mathrm{N}$ at a proton energy near the narrow resonance at $E_p = 629$ keV ($\Gamma = 2$ keV). For the measurements under the Al caps the proton beam energy was increased to take into account the energy loss of the incident protons in the Al layer. The nuclear reaction spectra corresponding to A_o and A_c are shown in Fig. 2. The α peak from A_o indicates the presence in the porous layer of ^{18}O atoms coming from the thermal oxidation. Because of the presence of the Al cap, the α peak from A_c is expected at an energy lower by 100 keV than that from the α peak from A_o. The counts from A_c and B_c which are 1 order of magnitude lower than that from A_o are equal, and hence correspond only to a background coming from nuclear reactions with silicon, boron atoms, etc. This experiment reveals that this medium is composed of noninterconnected single pores, the tops of which are in direct contact with the gas reservoir during adsorption.

Another important property of this medium is the constancy of the Si wall thickness revealed by the transmission electron microscopy (TEM) plane view performed on a porous layer thinned down to 1000 Å, i.e., about 10 times the size of the pores. This is a strong argument against the presence of narrow sections inside the pores, the presence of which would lead, through shadow effects, to an inhomogeneous apparent thickness of the Si walls.

The PSD of the porous Si layers has been estimated from a numerical treatment of the TEM images. The negative TEM photographs are digitized by means of a CCD camera. The value of the threshold to make the image binary is chosen to reproduce the porosity of the sample. Analysis of this binary image allows one to obtain the cross section area and perimeter of each pore. The PSD, which corresponds to cylindrical pores having the same cross section area as the polygonal pores, is shown in the inset of Fig. 1(a). The mean pore diameter is 13 nm with a standard deviation of ± 6 nm.

Nitrogen adsorption isotherms were measured by a volumetric technique up to the saturating vapor pressure of bulk nitrogen (P_0) and at 77 K. The samples were outgassed at ambient temperature for a few hours. This outgassing does not change the nearly complete passivation of the inner surface by a monolayer of $SiH_{1,2,3}$ groups which takes place during the electrochemical etching and which is stable for a few days after the formation [7].

Figure 3(a) shows N_2 adsorption isotherms at 77 K corresponding to porous Si layers with pores open at one or at both ends, the PSD of which is represented in the inset of Fig. 1(a). These two curves exhibit wide and asymmetrical hysteresis loops with shapes corresponding to type H2 (1985 IUPAC classification [8]) or type E [9].

The adsorbed amount of gas sharply increases between 0.55 and $0.8P_0$ and then reaches a plateau region where all the pores are filled with the dense phase. The steep desorption process occurs over a pressure range about 3 times narrower than that of the adsorption.

Assuming that the density of the dense phase equals that of bulk liquid nitrogen, the pore volume extracted from the value of the adsorbed amount on the plateau region is in very good agreement with that measured by gravimetry.

Cohan's model predicts that, for a cylindrical pore open at both ends, condensation takes place at a pressure P_c given by an equation similar to the classical Kelvin equation where the curvature of the meniscus is replaced by a cylindrical curvature:

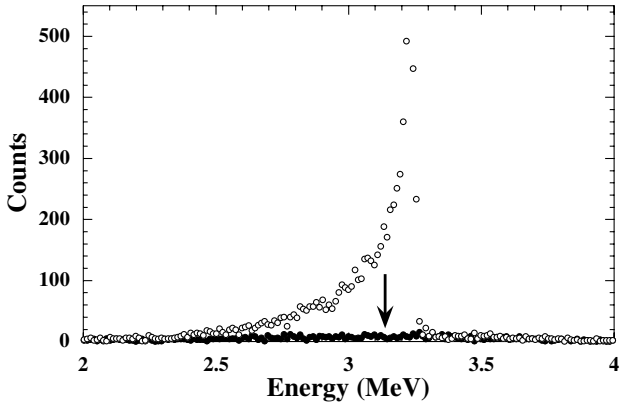

FIG. 2. α spectra from $^{18}O(p,\alpha)^{15}N$: $E_p = 629$ keV. ($\circ$) Porous Si layer after thermal oxidation in $^{18}O_2$ (A_o). ($\bullet$) Part of the layer protected by Al cap (A_c). The arrow indicates the energy of the expected α peak from A_c.

$$\ln\left(\frac{P_c}{P_0}\right) = -\frac{\sigma V_L}{RT[r - t(P_c)]}, \quad (1)$$

where V_L is the molar liquid volume, σ is the liquid-gas surface tension at temperature T, r is the radius of the pore, and $t(P)$ is the thickness of the adsorbed layer at P. For a cylindrical pore closed at one end, surface thermodynamic considerations predict a preferential adsorption on the bottom of the pore; a hemispherical meniscus is then present provided that there is perfect wetting, so that the condensation occurs at a pressure P_h given by the following modified Kelvin equation:

$$\ln\left(\frac{P_h}{P_0}\right) = -\frac{2\sigma V_L}{RT[r - t(P_h)]}. \quad (2)$$

The evaporation of the wetting fluid proceeds through the same hemispherical meniscus in both cases, i.e., at the same pressure P_h.

Thus, according to Cohan's model: (i) the adsorption should be reversible in a pore open at one end but irreversible in a pore open at both ends; (ii) the adsorption branch for a pore open at both ends should be located at a pressure (P_c) higher than that for a pore closed at one end (P_h); (iii) for a given size distribution of cylindrical pores open at both ends, the adsorption branch should be steeper than the desorption branch (provided that the diameter exceeds 3–4 nm) and the shape of the hysteresis loop becomes rather symmetrical as the pore diameter increases, as shown by numerical calculations based on Eqs. (1) and (2) in which we have introduced a currently used $t(P)$ proposed by Halsey [10,11] or the $t(P)$ reproducing our experimental values prior to the capillary condensation.

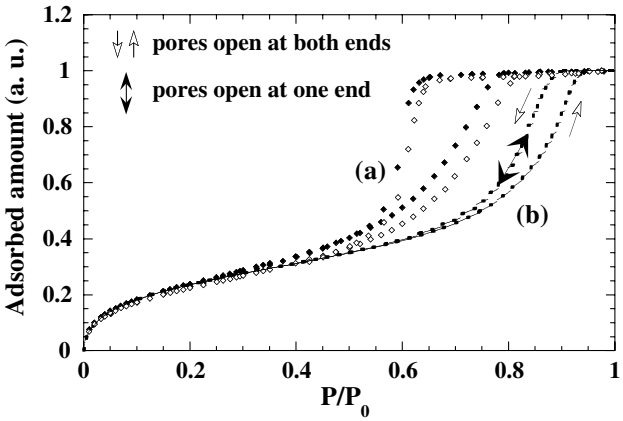

FIG. 3. (*a*) N_2 adsorption isotherms at 77 K for porous Si with pores open at one ($\blacklozenge$) or at both ($\diamond$) ends. (*b*) Isotherms calculated by introducing in Eqs. (1) and (2) the experimental $t(P)$ values (see text) and the PSD shown in Fig. 1.

To extract the latter $t(P)$ values, we prepared a porous Si layer with a PSD having a mean value as high as possible (about 50 nm) in order to shift the capillary condensation pressures to the highest possible values. The obtained isotherm exhibits hysteresis loop located above $0.8P_0$. We have thus determined the numerical values of $t(P)$ up to $0.8P_0$ by assuming (A) that the density of the adsorbate equals that of bulk liquid nitrogen, (B) a cylindrical shape for the pores, the PSD of which was extracted as explained above, and (C) that $t(P)$ is independent of the pore radius. For $t(P)$ above $0.8P_0$, we have chosen to extrapolate the polynomial law which fits the experimental $t(P)$. The isotherm calculated by introducing in Eqs. (1) and (2) the $t(P)$ and the PSD shown in the inset of Fig. 1(a) is represented Fig. 3(*b*).

We will successively discuss predictions (i) and (iii) which are in large discrepancy with the experimental results [Fig. 3(*a*)]; prediction (ii) which is in agreement with experiment, and finally, the large shift between the absolute position of the experimental isotherms and the calculated ones.

Prediction (i): The adsorption-desorption cycle observed in the case of pores closed at one end is irreversible. The interconnectivity related pore blocking effect described by Mason [12] to explain the origin of the hysteresis phenomenon could not occur because the porous Si layers are composed of noninterconnected pores. Moreover, we reject the "ink bottle" effect, introduced by Everett [13], as a possible explanation of the isotherm hysteresis loop we observe because of the absence of narrow sections inside the pores.

Prediction (iii): The hysteresis loops observed in the porous layer and porous membrane exhibit the same shape of type H2. We have observed, by carrying out adsorption isotherms on porous Si layers with a PSD having mean values varying from 13 nm up to 50 nm, that the position on the pressure axis of the corresponding adsorption and desorption branches are shifted towards P_0 whereas the shape of the hysteresis loops remains of type H2.

Such asymmetry is not expected by the single pore models. Indeed, numerical calculations based on Cohan's model or on DFT [14] predict a symmetrical shape of the hysteresis loop for such large pores, in contradiction with what we observe. Furthermore, although porous Si exhibits noninterconnected pores, the hysteresis shape (type H2) we observe is the same as those systematically

obtained for highly interconnected mesoporous solids such as controlled pore glass or Vycor [15]. From a theoretical viewpoint, both macroscopic [12] and microscopic [14] approaches described this shape as a signature of the disorder introduced by the interconnectivity between pores. We must conclude that type H2 hysteresis is not characteristic of interconnected porous materials and we thus reject the conclusion made by Ball and Evans [14] according to which a de Boer's shape of hysteresis is a consequence of an interconnected network effect.

We believe that the desorption process we observe results from another effect. At the end of the adsorption process, pores are filled by the dense phase and the external surface of the porous layer is covered by a film which connects the pores. This film could play an important role in the desorption process by preventing the concave menisci from passing through each pore at the expected equilibrium pressure, the emptying of the pores being controlled by the tearing of the film at the edges of the pores. The steepness of the desorption branch could be explained if the tearing of the film occurs at a pressure lower than the equilibrium pressures corresponding to the hemispherical menisci of the major proportion of the pores. We note that the desorption of such a more realistic system, which consists of a fluid filling and covering pores of finite length with edges at their open ends, has never been studied.

Note that the analysis of the desorption branch using the BJH method yields a PSD with a width about 0.5 nm which is very far from that of the actual PSD (± 6 nm) [16]. It is conventionally admitted [14,17] that the desorption process in porous materials occurs at the coexistence of high and low dense phases. On such an assumption, a steep desorption branch is interpreted as the signature of the presence of pores of a unique size [18]. Our results obviously show that it is not necessarily the case.

Prediction (ii): The sign of the relative positions of the two adsorption branches ($P_h < P_c$) is in agreement with Cohan's model. These experiments reveal two different scenarios for the filling of pores open at one or at both ends. Preferential adsorption in the bottom of closed pores is confirmed by analytical calculations performed in an oblique corner formed by the intersection of two planar surfaces [19]. We are currently investigating the pore closure effect on adsorption in cylindrical geometry by means of GCMC simulations and DFT calculations.

As shown in Fig. 3(*b*), the curve which corresponds to the modified Kelvin equation (2) is largely outside the experimental hysteresis loops. For pore sizes as large as in our samples, this equation should account for the equilibrium phase transition. Indeed, microscopic calculations based on DFT performed by Ball and Evans [14] have shown that, in the case of a distribution of cylindrical pores open at both ends centered on 7.2 nm, which is 2 times smaller than the mean size of our pores, the coexistence curve is located at a pressure close to that predicted by Eq. (2). To our knowledge, this is the first time that, for such large pores, such a large discrepancy is found [20]. This may be due to the use of a cylindrical geometry in the calculations which does not account for the actual polygonal shape of pores. GCMC simulations and DFT based calculations are in progress.

In summary, we have studied the adsorption phenomenon in a porous Si medium, a well-ordered material with tubular pores without narrow sections and for which we have experimentally proven the absence of interconnection. Type H2 hysteresis is observed whether the pores are open at one or at both ends. These results are in contradiction with Cohan's model and show that the sole observation of type H2 hysteresis is not the signature of the presence of interconnections in porous material as is generally believed. The steep desorption process cannot be described by the macroscopic Kelvin equation in which we introduce the experimental values of the thickness of adsorbed film prior to the capillary condensation. We note that the application of the widely used BJH method to extract the PSD from this branch is not systematically justified.

We thank N. Dupont-Pavlovsky and Professor X. Duval for fruitful discussions and T. McRae for careful reading of the manuscript.

[1] R. Zsigmondy, Z. Anorg. Allgem. Chem. **71**, 356 (1911).
[2] L. H. Cohan, J. Am. Chem. Soc. **60**, 433 (1938).
[3] A. Papadopoulou, F. Van Swol, and U. Marini Bettolo Marconi, J. Chem. Phys. **97**, 6942 (1992).
[4] F. Celestini, Phys. Lett. A **228**, 84 (1997).
[5] R. Evans, U. Marini Bettolo Marconi, and P. Tarazona, J. Chem. Phys. **84**, 2376 (1986).
[6] E. P. Barrett, L. G. Joyner, and P. H. Halenda, J. Am. Chem. Soc. **73**, 373 (1951).
[7] A. Grosman and C. Ortega, in *Structural and Optical Properties of Porous Silicon Nanostructures,* edited by G. Amato, C. Delerue, and H. Von Bardeleben (Gordon and Breach, New York, 1997), Chap. 11, pp. 317–332; *ibid.*, Chap. 13, pp. 375–408.
[8] K. S. W. Sing *et al.,* Pure Appl. Chem. **57**, 603 (1985).
[9] J. H. de Boer, in *The Structure and Properties of Porous Materials,* edited by D. H. Everett and F. S. Stone (Butterworths, London, 1958), p. 68.
[10] G. Halsey, J. Chem. Phys. **16**(10), 931 (1948).
[11] S. J. Gregg and K. S. W. Sing, in *Adsorption, Surface Area and Porosity* (Academic Press, London, 1982).
[12] G. Mason, J. Colloid Interface Sci. **88**, 36 (1982).
[13] D. H. Everett, in *The Structure and Properties of Porous Materials* (Ref. [9]), p. 95; J. A. Barker *ibid.*, p.125.
[14] P. C. Ball and R. Evans, Langmuir **5**, 714 (1989).
[15] A. J. Brown, Ph.D. thesis, University of Bristol, 1963.
[16] B. Coasne *et al.,* Phys. Chem. Chem. Phys. **3**, 1196 (2001).
[17] W. F. Saam and M. W. Cole, Phys. Rev. B **11**, 1086 (1975).
[18] S. Gross and G. H. Findenegg, Ber. Bunsen-Ges. Phys. Chem. **101**, 1726 (1997).
[19] E. Cheng and M. W. Cole, Phys. Rev. B **41**, 9650 (1990).
[20] L. D. Gelb, K. E. Gubbins, R. Radhakrishnan, and M. Sliwinska-Bartkowiak, Rep. Prog. Phys. **62**, 1573 (1999).